J Solid State Electrochem (2012) 16:1901–1906
DOI 10.1007/s10008-011-1591-5

ORIGINAL PAPER

Preparation and electrocatalytic performance of Fe–N–C for electroreduction of H_2O_2

Yongmei Tian · Jichun Huang · Yuan Gao · Dianxue Cao · Guiling Wang

Received: 11 July 2011 / Revised: 1 November 2011 / Accepted: 6 November 2011 / Published online: 26 November 2011

Abstract Fe–N–C catalysts were prepared through metal-assisted polymerization method. Effects of carbon treatment, Fe loading, nitrogen source, and calcination temperature on the catalytic performance of the Fe–N–C for H_2O_2 electroreduction were measured by voltammetry and chronoamperometry. The Fe–N–C catalyst shows optimal performance when prepared with pretreated active carbon, 0.2 wt.% Fe, paranitroaniline (4-NA) and one-time calcination. The Fe–N–C catalyst displayed good performance and stability for electroreduction of H_2O_2 in alkaline solution. An Al–H_2O_2 semi-fuel cell was set up with Fe–N–C catalyst as cathode and Al as anode. The cell exhibits an open-circuit voltage of 1.3 V and its power density reached 51.4 mW cm^{-2} at 65 mA cm^{-2}.

Keywords Fe-based catalysts · Hydrogen peroxide electroreduction · Fuel cell

Introduction

In recent years, fuel cells using hydrogen peroxide oxidant have received considerable attention. These fuel cells include direct borohydride–hydrogen peroxide fuel cell [1–6], metal–hydrogen peroxide semi-fuel cell [7–13], hydrazine–hydrogen peroxide fuel cell [14], and direct methanol–hydrogen peroxide fuel cell [15–17]. They generally have high energy density, high performance, compact design, and workability in environments without air. Therefore, they are good candidates of underwater and space powers.

Hydrogen peroxide has the following advantages when used as oxidant of fuel cells: (1) Hydrogen peroxide is in liquid form; compared with oxygen gas, it has high volume energy density and its handling, storage, and feeding to a fuel cell are easy. (2) The electroreduction of hydrogen peroxide is a two-electron transfer process and hence has lower activation energy. The exchange current density of hydrogen peroxide reduction is around six orders higher than that of oxygen reduction. (3) The electroreduction of liquid hydrogen peroxide on a fuel cell cathode occurs in a solid/liquid two-phase reaction zone, while oxygen electroreduction requires a solid/liquid/gas three-phase region. The two-phase reaction zone is readily realizable and much steady during fuel cell operation than the three-phase region.

Four types of electrocatalysts for hydrogen peroxide reduction have been reported. They are (1) noble metals, such as platinum, palladium, iridium, silver, gold, and a combination of these [1, 5, 7, 10–12]; (2) macrocycle complexes of transition metals, such as Fe- and Co-porphyrin, Cu-triazine complexes [18, 19]; (3) metallic oxide, such as cobalt oxide [6, 20, 21]; and (4) perovskite [22].

Jasinski et al. [23] reported the first oxygen reduction reaction (ORR) catalyst with macrocyclic structure containing nitrogen–metal coordination in 1964. Carbon-supported metal N4-macrocycles are generally prepared via pyrolysis method [24] and are primarily used as oxygen electroreduction catalyst for proton exchange membrane (PEM) fuel cells [19, 23–26] and also investigated as catalysts for

Y. Tian · J. Huang · Y. Gao · D. Cao · G. Wang (✉)
Key Laboratory of Superlight Material and Surface Technology of Ministry of Education, College of Material Science and Chemical Engineering, Harbin Engineering University,
Harbin, 150001 People's Republic of China
e-mail: wangguiling@hrbeu.edu.cn

Y. Tian
School of Chemistry and Materials Science,
Heilongjiang University,
Harbin, 150080 People's Republic of China

H_2O_2 electroreduction. Raman et al. [18] investigated FeTMPP/C as the cathode catalyst for direct borohydride–hydrogen peroxide fuel cell. They observe a maximum power density of 82 mW cm^2 at cell potentials of 0.5 V and at 70 °C. However, the effects of different preparation conditions on the catalytic performance of the Fe–N–C for H_2O_2 electroreduction are unclear.

In this study, Fe–N–C catalysts were prepared through metal-assisted polymerization of nitrogen-containing aromatic molecules. The results indicated that Fe–N–C catalyst is an attractive candidate of low-cost electrocatalyst for H_2O_2 reduction.

Experimental

The Fe–N–C catalyst was synthesized according to the modified procedures described in the literature [25]. In a typical preparation, the anhydrous iron chloride was mixed with nitroaniline and active carbon (2,600 m^2 g^{-1}) by ball-milling at 400 rpm for 10 h. The mixture was first heated to 160 °C in nitrogen atmosphere under stirring to melt nitroaniline and further homogenize the reactants and then heated to 200 °C to induce the polymerization reaction accompanying with gas evolution. After the gas evolution subsides, the mixture was heated to 300 °C to ensure complete polymerization and then calcined at 950 °C under flowing nitrogen and ammonia. The obtained catalysts, after ball-milling, were washed with 2 mol L^{-1} H_2SO_4 to remove the leachable Fe species, further washed with distilled water extensively to remove chloride and sulfate ions, and dried at 70 °C in a vacuum oven for 4 h.

Fe–N–C electrodes were prepared as follows: Fe–N–C powder was dispersed in anhydrous ethanol and sonicated for 5 min to obtain a suspension, into which a PTFE emulsion was added. The mixture was sonicated for 20 min and then heated at 80 °C until a thick paste was formed. The paste was filled in pores of nickel foam, heated at 110 °C for 12 h in a vacuum oven, and pressed at 10 MPa. The final electrodes (denoted as Fe–N–C/ Ni-foam) have a catalyst loading of 13 mg cm^{-2}. The ratio of Fe–N–C to PTFE is 4:1. The morphology was examined by scanning electron microscope (SEM; JEOL JSM-6480) attached to an energy-dispersive X-ray analyzer. Electrochemical measurements were performed in a conventional three-electrode electrochemical cell using a computerized VMP3/Z potentiostat (Bio-Logic) controlled by the EC-lab software. The catalyst performance was investigated by cyclic voltammogram (CV) and chronoamperometric curves in 3 mol L^{-1} KOH and 0.6 mol L^{-1} H_2O_2 electrolyte. The prepared electrode (1 cm^2 nominal planar area) acted as the working electrode, a platinum foil (1×2 cm^2) served as the counter electrode, and a saturated Ag/AgCl was used as the reference electrode.

The performance of the Al–H_2O_2 semi-fuel cell was examined using a home-made flow through test cell made of stainless steel equipped with heating blocks. The anode is pure aluminum (99.9%, 20×20×0.5 mm), and the cathode was the prepared Fe–N–C/Ni-foam electrode. Nafion-115 (DuPont, USA) membrane was used to separate the anode and the cathode compartments. Prior to use, the membrane was pretreated by boiling in 3% H_2O_2 for 1 h and in ultrapure water for 2 h and then soaking in 2.0 mol L^{-1} KOH for 1 h. The anolyte (3.0 mol L^{-1} KOH) and the catholyte (3.0 mol L^{-1} KOH and H_2O_2) were pumped into the bottom of the anode and the cathode compartments, respectively, by their individual peristaltic pump and exited at the top of the compartments. The flow rate is 80 mL min^{-1} for both the anolyte and the catholyte. The discharge performance of the Al–H_2O_2 semi-fuel cell was measured using a computer-controlled E-load system (Arbin, USA).

Results and discussion

Characterization of the Fe–N–C catalyst

Figure 1 shows the SEM image and the corresponding C, N, and Fe elemental mappings of Fe–N–C catalyst. It is evident from Fig. 1c, d that the transition metal compounds were derived by paranitroaniline and Fe, but the structure of Fe–N–C catalyst is not certain. In the last several years, numerous articles discussing the Fe-based catalysts have been published, including an excellent review by Dodelet [27] where both the developments leading to and the work most relevant to our own approach are summarized in a comprehensive way. Dodelet's group produced time-of-flight secondary ion mass spectroscopy data and X-ray photoelectron spectroscopy spectra from which they proposed that the composition of the most catalytically active functional group is Fe–N_2–C_x [28].

Parameters affecting catalyst activity for H_2O_2 electroreduction

In this section, we present data showing the performance of Fe–N–C catalyst derived from active carbon, Fe loading, nitrogen source, calcination times, and H_2O_2 concentration leading to the most active catalysts.

The effect of carbon treatment

The surface properties of the carbon support have a significant effect on the degree of catalyst dispersion [24]. Earlier studies [29] have demonstrated that the carbon support plays an important role in improving the activity

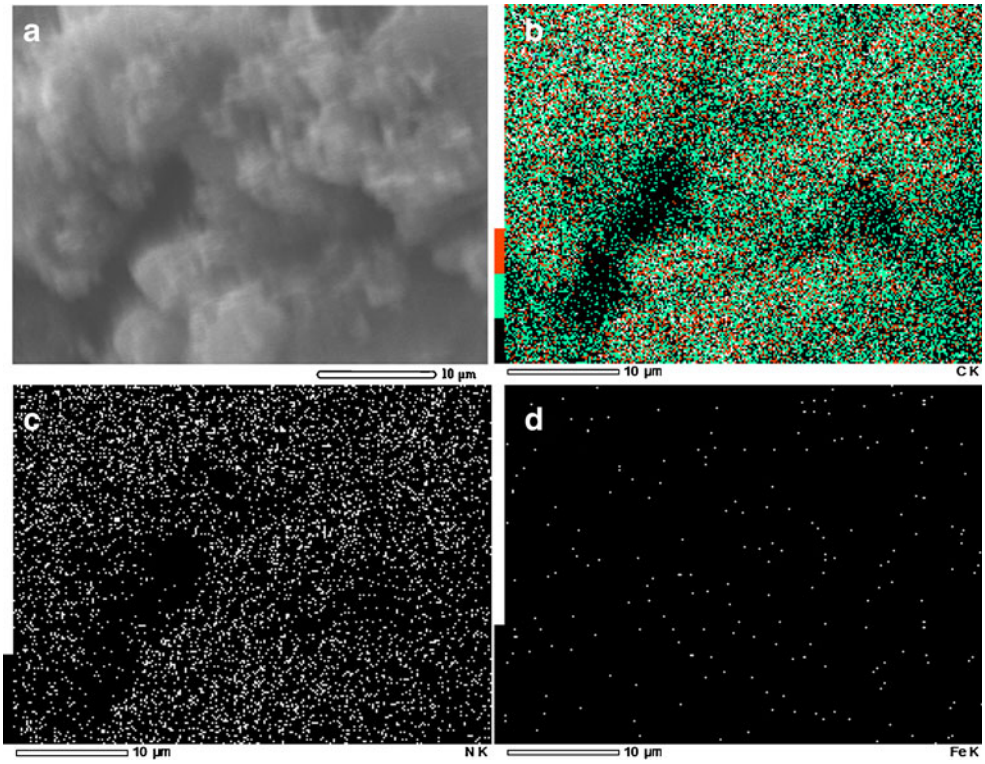

Fig. 1 **a** SEM image and the corresponding elemental distributions of **b** C, **c** N, and **d** Fe of Fe–N–C catalyst

and stability of heat-treated metal macrocycles. Figure 2 shows the effects of the active carbon treatments on the catalyst performance. Curve a represents the pristine active carbon and curve b represents the active carbon pretreated by 2 mol L^{-1} HCl. The current density at −0.3 V reached 19.2 and 47.3 mA cm^{-2} for untreated and treated active carbon, respectively. The limiting diffusion current reached 41.6 and 82.8 mA cm^{-2} for pristine and HCl-treated active carbon, respectively. These results demonstrated that the catalytic performance of Fe–N–C/Ni-foam electrode was improved when active carbon was pretreated with HCl. The acid treatment of active carbon might increase the porosity and enlarge the specific surface by removing impurities [24, 26].

The effect of Fe loading

Figure 3 shows the effects of Fe loading on catalyst performance. It can be seen that when the weight content of Fe is 0.0%, 0.2%, and 0.3%, the current density at −0.3 V reached 32.0, 47.1, and 34.5 mA cm^{-2}, respectively. The limiting diffusion current reached 61.6, 82.9, and 70.3 mA cm^{-2} for the catalyts containing 0.0%, 0.2%, and 0.3% Fe, respectively. Clearly, the addition of Fe enhanced the catalytic performance for H_2O_2 electroreduction, and 0.2% Fe shows better performance than others. Bezerra et al. [24] studied the effect of Fe loading on electrocatalyst activity under the same conditions for ORR. They concluded that when the loading reaches a certain level, a saturated activity level (a plateau) can be observed. When the loading is overloaded, the activity falls dramatically. Because of the oxygen reduction process, the following two steps might exist: (1) from O_2 to H_2O_2 and (2) from H_2O_2 to H_2O [19]. To some extent, the conclusion summarized by Bezerra et al. [24] might also explain our results.

The effect of nitrogen source

Nitrogen is a necessary component of the catalytic active sites [30, 31]. Figure 4 shows the effects of nitrogen source

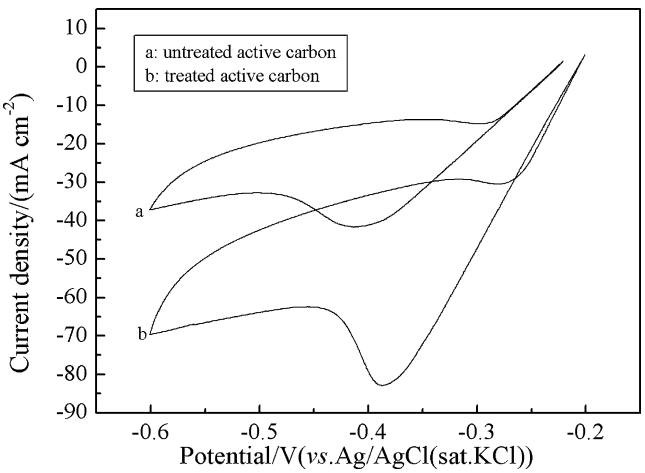

Fig. 2 Effects of active carbon treatment on catalyst performance. (Preparation parameters: 0.2 wt.% Fe, 4-NA, calcination once) The scan rate is 5 mV s^{-1}

on catalyst performance. Nitroaniline (2-NA) and para-nitroaniline (4-NA) were investigated as the nitrogen sources. As can be seen from Fig. 3, the current density at −0.3 V reached 28.2 and 47.1 mA cm^{-2} for catalyst resulted from 2-NA and 4-NA, respectively. The limiting diffusion current reached 52.6 and 82.9 mA cm^{-2} for 2-NA and 4-NA, respectively. So, 4-NA is a better nitrogen source than 2-NA. Wood et al. [25] studied the catalytic activity of 2-NA and 4-NA-derived catalyst materials as cathode for PEM fuel cells. They also provide a notable example of where small changes in the structure of a precursor molecule produce marked differences in the electrochemical properties of the resulting catalysts despite the fact that the catalysts were derived from high-temperature pyrolysis in reactive gas.

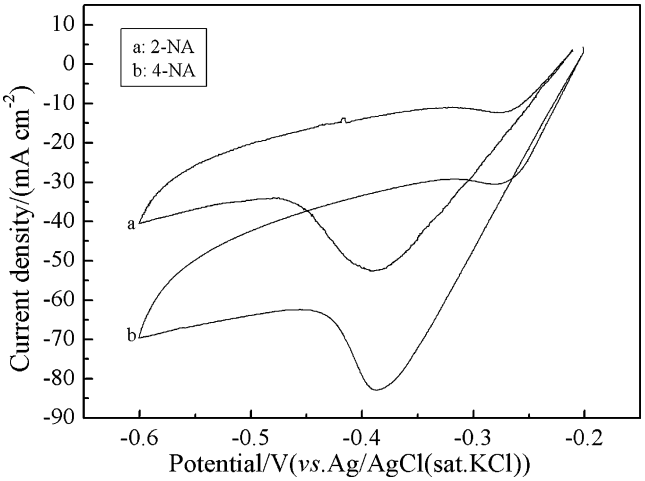

Fig. 4 Effects of nitrogen source on catalyst performance. (Preparation parameters: 0.2 wt.% Fe, pretreated active carbon, calcination once) The scan rate is 5 mV s^{-1}

The effect of calcination times

Despite decades of research on heat-treated Fe- and Co-based ORR catalysts, the nature of active sites are still not quite clear. However, there is general agreement in literatures that a heat-treatment step has beneficial effects on both the activity and the stability of these electrocatalysts [24]. Figure 5 shows the effects of calcination times on catalyst performance. The current density at −0.3 V reached 33.0 and 43.7 mA cm^{-2} for catalyst resulted from two- and one-time calcination, respectively. The limiting diffusion current reached 66.1 and 77.8 mA cm^{-2} for two- and one-time calcination, respectively. These results demonstrated that one-time calcination shows better performance than two-time calcination. Veen et al. [32] concluded the calcination conditions in an effort to explain this effect: (1) catalyzing the formation of a special type of carbon, which is actually the active phase, and (2) promoting a reaction between chelate and subjacent carbon in such a way as to modify the electronic structure of the central metal ion with retention of its N_4-coordinated environment. However, the true causes and mechanisms are still not fully understood.

The effect of H_2O_2 concentration

Figure 6 shows the effects of hydrogen peroxide concentration on the catalytic behavior of Fe–N–C/Ni-foam electrode. The limiting diffusion current reached 39.5, 61.1, 76.4, 93.3, and 108.0 mA cm^{-2} for the H_2O_2 concentration of 0.2, 0.4, 0.6, 0.8, and 1.0 mol L^{-1}, respectively. It was found that cathodic peak currents increased approximately linearly with the increase of

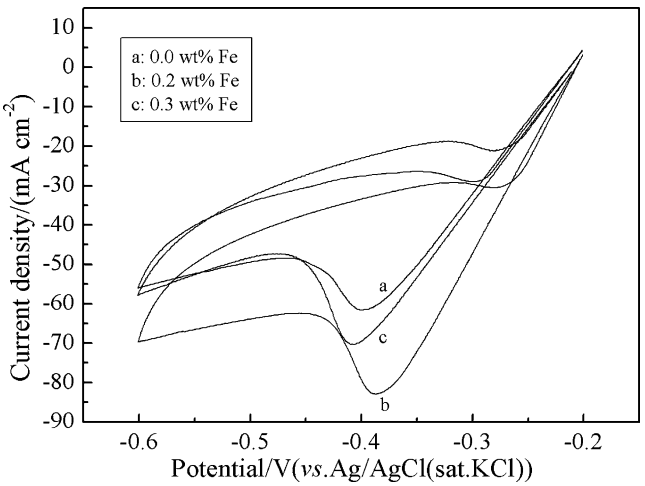

Fig. 3 Effects of Fe loading on catalyst performance. (Preparation parameters: 4-NA, pretreated active carbon, calcination once) The scan rate is 5 mV s^{-1}

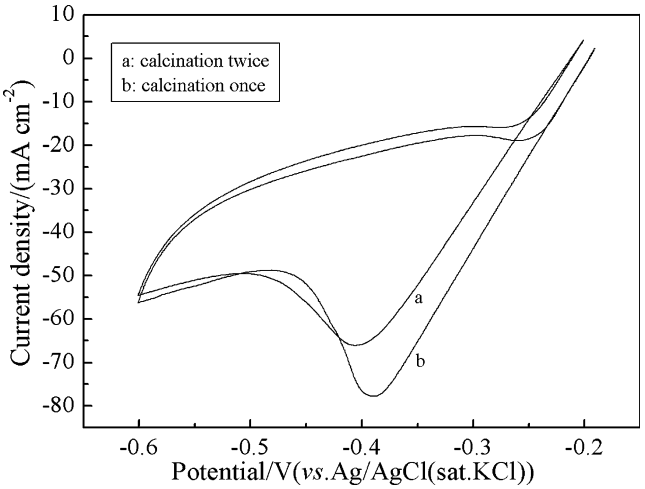

Fig. 5 Effects of calcination times on catalyst performance. (Preparation parameters: 0.2 wt.% Fe, 4-NA, pretreated active carbon) The scan rate is 5 mV s^{-1}

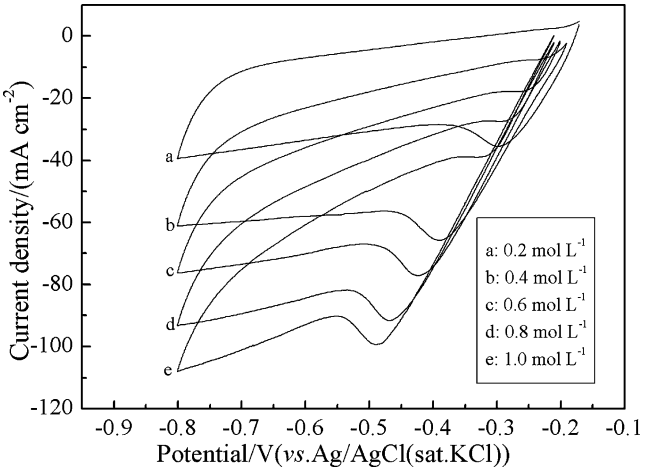

Fig. 6 CVs of Fe–N–C/Ni-foam electrode measured in 3.0 mol L^{-1} KOH containing H_2O_2 with different concentrations between 0.2 and 1.0 mol L^{-1}. (Preparation parameters: 0.2 wt.% Fe, 4-NA, pretreated active carbon, calcination once) The scan rate is 5 mV s^{-1}

H_2O_2 concentration from 0.2 to 1.0 mol L^{-1}, demonstrating that the reduction reaction at the peak potential is diffusion-controlled. When the H_2O_2 concentration increased to 0.8 mol L^{-1}, the cathodic peak currents increased conspicuously and the decomposition of H_2O_2 was observed (indicated by the formation of small bubbles on the electrode surface) during the test. A current density of 108.0 mA cm^{-2} was achieved at 1.0 mol L^{-1} H_2O_2, of course at the expense of significant H_2O_2 decomposition.

Figure 7 demonstrates chronoamperometric curves for hydrogen peroxide reduction measured in 3.0 mol L^{-1} KOH containing 0.6 mol L^{-1} H_2O_2. At the mixed kinetic–diffusion control potentials (−0.3 V), currents reached a steady state after a few seconds and displayed no decrease within 30 min of test period, indicating that the Fe–N–C/Ni foam has good stability for hydrogen peroxide reduction in alkaline electrolyte.

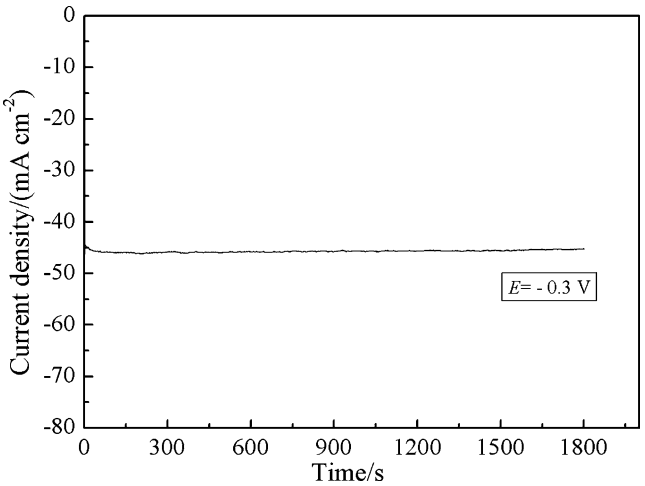

Fig. 7 Chronoamperometric curves for H_2O_2 reduction at −0.3 V in 3.0 mol L^{-1} KOH+0.6 mol L^{-1} H_2O_2

Performance of Al–H_2O_2 semi-fuel cell

Figure 8 shows the cell voltage and power density versus current density curves recorded with varying concentrations of H_2O_2 feeding to the cathode compartment. An open-circuit voltage of around 1.3 V was obtained. The cell voltage decays linearly with the increase of current density until reaching the mass transport control region, then it drops slowly. This indicated that cell performance can be dependent on the ohmic resistance of the cell. The increase of H_2O_2 concentration did not significantly affect the linear portion of the polarization curves but led to a significant increase in mass transport limiting currents. For example, the limiting current density increased from 38 mA cm^{-2} at 1.0 V to 65 mA cm^{-2} at 0.8 V when the concentration of H_2O_2 increased from 0.2 to 0.8 mol L^{-1}. Decomposition of H_2O_2 occurred at a concentration higher than 0.8 mol L^{-1}; in fact, it affected cell performance. The power density–current density curves exhibited maximum power densities of 51.4 mW cm^{-2} at 65 mA cm^{-2}, operating on 0.6 mol L^{-1} H_2O_2.

Conclusions

Fe–N–C catalyst was synthesized and its performance as H_2O_2 electroreduction catalyst was investigated. It was found that Fe–N–C/Ni foam electrode displayed good stability for H_2O_2 electroreduction in alkaline electrolyte. An Al–H_2O_2 semi-fuel cell using Fe–N–C as the cathode catalyst displayed an open-circuit voltage of 1.3 V and peak power density of 51.4 mW cm^{-2} at 65 mA cm^{-2}, operating on 0.6 mol L^{-1} H_2O_2. This study shows that Fe–N–C is an attractive candidate for solving the problem of the cost of fuel cell catalysts.

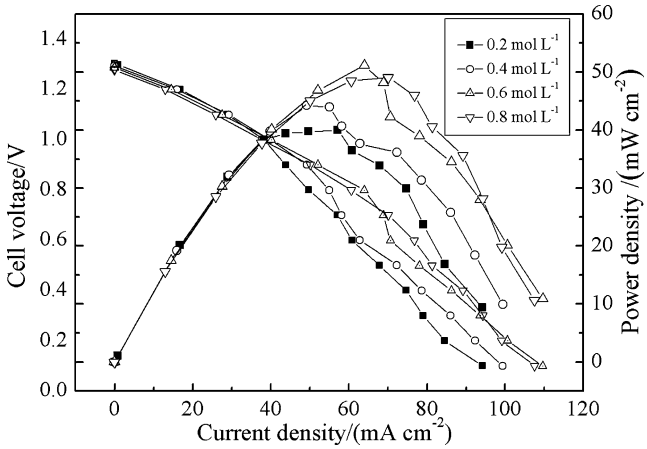

Fig. 8 Performance of Al–H_2O_2 semi-fuel cell with Fe–N–C/Ni-foam cathode operating at room temperature. The catholytes are 3.0 mol L^{-1} KOH containing H_2O_2 with different concentrations. (Preparation parameters: 0.2 wt.% Fe, 4-NA, pretreated active carbon, calcination once)

Acknowledgements We gratefully acknowledge the financial support of this research by National Nature Science Foundation of China (20973048).

References

1. de León CP, Walsh FC, Rose A, Lakeman JB, Browning DJ, Reeve RW (2007) J Power Sources 164:441–448
2. Miley GH, Luo N, Mather J, Burton R, Hawkins G, Gu L, Byrd E, Gimlin R, Shrestha PJ, Benavides G, Laystrom J, Carroll D (2007) J Power Sources 165:509–516
3. Raman RK, Prashant SK, Shukla AK (2006) J Power Sources 162:1073–1076
4. Choudhury NA, Raman RK, Sampath S, Shukla AK (2005) J Power Sources 143:1–8
5. Gu L, Luo N, Miley GH (2007) J Power Sources 173:77–85
6. Cao D, Chen D, Lan J, Wang G (2009) J Power Sources 190:346–350
7. Bessette RR, Medeiros MG, Patrissi CJ, Deschenes CM, LaFratta CN (2001) J Power Sources 96:240–244
8. Dow EG, Bessette RR, Seeback GL, Marsh-Orndorff C, Meunier H, VanZee J, Medeiros MG (1997) J Power Sources 65:207–212
9. Medeiros MG, Bessette RR, Deschenes CM, Patrissi CJ, Carreiro LG, Tucker SP, Atwater DW (2004) J Power Sources 136:226–231
10. Yang W, Yang S, Sun W, Sun G, Xin Q (2006) J Power Sources 160:1420–1424
11. Medeiros MG, Bessette RR, Deschenes CM, Atwater DW (2001) J Power Sources 96:236–239
12. Bessette RR, Cichon JM, Dischert DW, Dow EG (1999) J Power Sources 80:248–253
13. Hasvold Ø, Storkersen NJ, Forseth S, Lian T (2006) J Power Sources 162:935–942
14. Urbach HB, Bowen RJ (1970) J Electrochem Soc 117:1594–1600
15. Sung W, Choi J-W (2007) J Power Sources 172:198–208
16. Bewer T, Beckmann T, Dohle H, Mergel J, Stolten D (2004) J Power Sources 125:1–9
17. Prater DN, Rusek JJ (2003) Applied Energy 74:135–140
18. Raman RK, Shukla AK (2005) J Appl Electrochem 35:1157–1161
19. Liu H, Zhang L, Zhang J, Ghosh D, Jung J, Downing BW, Whittemore E (2006) J Power Sources 161:743–752
20. Wang G, Cao D, Yin C, Gao Y, Yin J, Cheng L (2009) Chem Mater 21:5112–5118
21. Cao D, Chao J, Sun L, Wang G (2008) J Power Sources 179:87–91
22. Wang G, Bao Y, Tian Y, Xia J, Cao D (2010) J Power Sources 195:6463–6467
23. Jasinski R (1964) Nature 201:1212–1213
24. Bezerra CWB, Zhang L, Lee K, Liu H, Marques ALB, Marques EP, Wang H, Zhang J (2008) Electrochim Acta 53:4937–4951
25. Wood TE, Tan Z, Schmoeckel AK, O'Neill D, Atanasoski R (2008) J Power Sources 178:510–516
26. Nallathambi V, Lee J-W, Kumaraguru SP, Wu G, Popov BN (2008) J Power Sources 183:34–42
27. Dodelet JP, Zagal J, Bedioui F, Dodelet JP (eds) (2006) N4-Macrocyclic metal complexes. Springer Science, New York
28. Lefèvre M, Dodelet JP (2000) J Phys Chem B 104:11238–11247
29. Widelöv A, Larsson R (1992) Electrochim Acta 37:187–197
30. Fournier J, Lalande G, Côté R, Guay D, Dodelet J-P (1997) J Electrochem Soc 144:218–226
31. Lalande G, Cote R, Guay D, Dodelet JP, Weng LT, Bertrand P (1997) Electrochim Acta 42:1379–1388
32. van Veen JAR, Colijn HA, van Baar JF (1988) Electrochim Acta 33:801–804